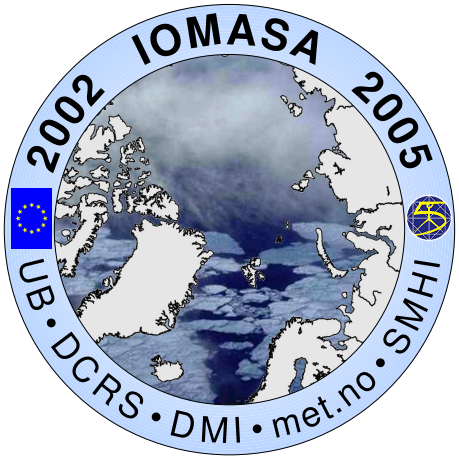

Report for IOMASA Deliverable 1.4b (IUP contribution): Validation of total water vapour algorithm

Christian Melsheimer, Georg Heygster

IUP, University of Bremen

Contents

1 Basic Algorithm

The total water vapour algorithm relies on a satellite radiometer (SSM/T2, AMSU-B) measurement of the brightness temperature at three different frequencies ν_i, ν_j, ν_k at which the ground emissivity ε is similar but the water vapour absorption is different, $\kappa_i < \kappa_j < \kappa_k$ (κ_i is the water vapour mass absorption coefficient at frequency ν_i).
The basic idea [Miao et al., 2001] is to use three channels where the surface emissivity is similar but the water vapour absorption is different, such as the three AMSU-B channels centred around the 183.3 GHz water vapour line.
Starting from the radiative transfer equation for a not too opaque atmosphere in the approximation of Guissard and Sobieski [1994], the following equation for the total water vapour W can be derived [Miao et al., 2001]:

$$W \sec\theta = C_0 + C_1 \log\left[\frac{T_i - T_j - F_y}{T_j - T_k - F_x}\right] \tag{1}$$

where θ is the viewing angle, T_i is the brightness temperature measured by AMSU-B at channel no. i, while the three channels i, j, and k are sorted in such a way that for the corresponding water vapour absorption coefficients, κ_i, κ_j, κ_k, we have $\kappa_i < \kappa_j < \kappa_k$. The four parameters C_0, C_1, F_x, F_y, which we shall call "calibration parameters", have to be determined empirically. To do this, radiosonde data (Arctic, 1997 till 2001, about 27000 profiles), were taken as input for simulating AMSU-B brightness temperatures with the radiative transfer model ARTS [The Atmospheric Radiative Transfer Simulator, see Buehler et al., 2005]), using a range of different surface emissivities between 0.6 and 0.96. In addition, from the humidity data of each radiosonde profile, the total water vapour was calculated directly. Several linear regressions then yield the four calibration parameters C_0, C_1, F_x, F_y [details: Miao, 1998].
Using the three channels near the water vapour line (AMSU-B channels 20, 19, and 18, i.e., $(i,j,k) = (20,19,18)$), the method works up to total water vapour contents of about 1.5 kg/m^2. If we replace the most water-vapour sensitive channel 18 by the window channel 17 at 150 GHz, i.e., $(i,j,k) = (17,20,19)$, the method works up to total water vapour contents of about 6 kg/m^2. Such water vapour values are typical for the Arctic ocean, Siberia and Northern Canada in winter, and for Greenland almost year-round. So, if we have determined those four calibration parameters, the TWV can be calculated from AMSU-B brightness temperatures without any further input.
In order to extend the retrieved water vapour range to higher values, the channel 19 is replaced by the window channel 16 at 89GHz, i.e., $(i,j,k) = (16,17,20)$. Since the emissivity of sea ice and ocean at 89GHz is significantly different from the emissivity at 150 and 183 GHz, the emissivity does not cancel out any more, and instead of (1), we get the "extended algorithm"

$$W \sec\theta = C_0 + C_1 \log\left(\frac{r_2}{r_1}\left[\frac{T_i - T_j - F_y}{T_j - T_k - F_x} + C\right] - C\right) \tag{2}$$

Here, $r_1 = 1 - \varepsilon_{89}$ and $r_2 = 1 - \varepsilon_{157}$ are the surface reflectivities, C depends on the water vapour absorption coefficients but can safely be approximated by 1 for TWV above 6 kg/m^2, and the other variables have the same meaning as in (1) above. This means that now, some information about the emissivity of sea ice at 89 and 150 GHz is needed. We have extracted this information from emissivity measurements over sea ice and open water during the SEPOR/POLEX (Surface Emissivities in Polar Regions-Polar Experiment; Selbach [2003]) campaign: Analysis of these data shows a moderately

high correlation of the emissivities ε_{89} and ε_{157} of sea ice at 89 and 150 GHz, respectively. A linear regression yields

$$\varepsilon_{89} = 0.1809 + 0.8192\varepsilon_{157} \tag{3}$$

where we have imposed the additional constraint that $\varepsilon_{89}(\varepsilon_{157} = 1) = 1$. Based on these data, the reflectivity ratio r_2/r_1 over sea ice can be approximated by a constant value of 1.22. This means that for the extended algorithm, we need, in addition to the four calibration constants, information on the sea ice cover. The algorithm is then applied over sea ice. Since the emissivity of open water is rather well known [English and Hewison, 1998], it is in principle possible to adapt the extended algorithm to the use over open water. However, we have not done this here since there are other remote sensing methods to retrieve TWV over open water, e.g., from other passive microwave sensors like SSM/I. Using this extended algorithm, the upper limit of the TWV that can be retrieved is about 12 kg/m^2. Thus, combining all three "sub-algorithms" mentioned so far (using channel triples 20,19,18; 17,20,19; 16,17,20), TWV values from 0 to at least 15 kg/m^2 can be retrieved from AMSU-B data, using three sets of the four calibration parameters. Each sub-algorithm is used as long as both the numerator and the denominator in (1) are negative.

2 Validation

The weighting functions of the AMSU-B channels as a function of total water vapour (TWV) in Figure 1 show roughly at which TWV values a channel is sensitive to water vapour. For example, the

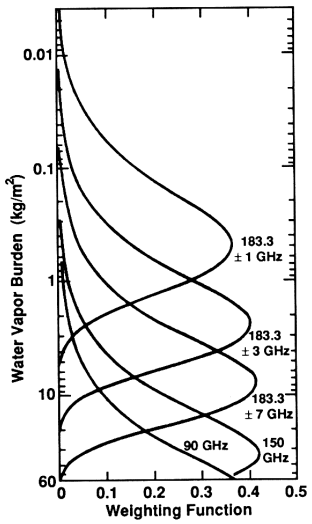

Figure 1: Weighting functions of AMSU-B channels as a function of total water vapour ("water vapour burden") over land, from Janssen [1993]

channel at 183.3±1 GHz (channel 18) is sensitive for TWV up to about 2 kg/m^2. For higher TWV, the weighting function rapidly approaches zero, in which case the channel is said to be saturated – thus, if there is so much water vapour that a channel is saturated, the radiation that the sensor measures does not come from the whole atmosphere any more, but only from an upper portion (the channel

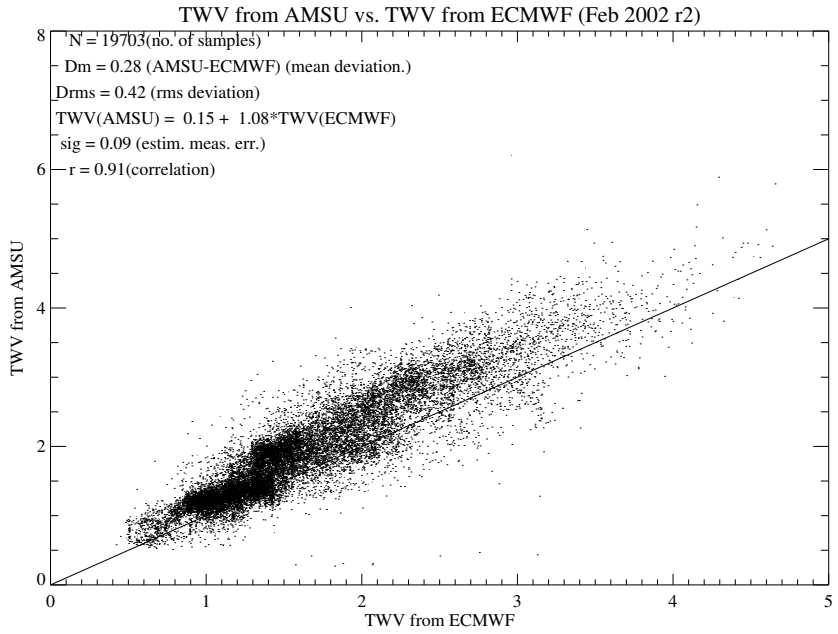

Figure 2: AMSU-B-derived TWV versus ECMWF (ERA-40) TWV. February 2002, North of Greenland (83–90°N, 0–90°W); solid line = identity.

"does not see the surface any more"). Channel 19 (183.3±3 GHz) saturates at around 8 kg/m^2 TWV (which roughly corresponds to the upper limit of the standard algorithm), channel 20 (183.3±7 GHz) saturates at around 20 kg/m^2 TWV - so we can expect the extended algorithm to retrieve water vapour roughly up to that value.

2.1 Direct comparison of collocated data

For validation purposes, the TWV data retrieved from AMSU-B data were compared to collocated ECMWF (European Centre for Medium-Range Weather Forecasts) reanalysis (ERA-40) data. For a typical winter month, February 2002, the result is shown in Figure 2. The correlation is 0.91, and the bias, i.e., the mean difference AMSU-derived minus ECMWF-reanalysis TWV, is about 0.31 kg/m^2. As seen in the plot, most TWV values are below 7 kg/m^2, so the standard algorithm has been used which is independent of surface emissivity.

The same comparison, but for a late summer month, August 2002, with minimum sea ice cover, is shown in Figure 3. Here, all values above 7 kg/m^2 have been retrieved using the extended algorithm. The correlation is only moderate, and the mean difference is much higher, about 2.7 kg/m^2. The reason is, of course, that the constant reflectivity ratio based on the regression analysis of SEPOR/POLEX data is only an approximation.

Comparison with TWV data derived from radiosonde measurements during Polarstern cruises is difficult since there is very little concurrent data, except for the cruise ARK XIX-1 (March-April 2003). The result of this comparison is shown in Figure 4. Here, the bias is positive as well, 1.3 kg/m^2, i.e., the AMSU-derived TWV values are higher than the ones derived from the radiosonde measurements. At least part of this positive bias can be explained by the fact that the radiosonde type used on Po-

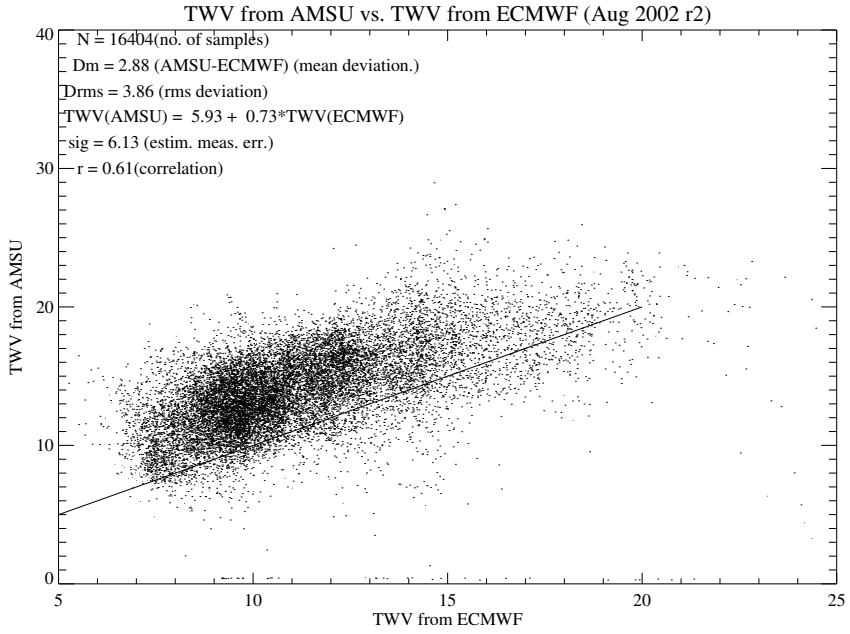

Figure 3: AMSU-B-derived TWV versus ECMWF (ERA-40) TWV. August 2002, North of Greenland (83–90°N, 0–90°W); solid line = identity.

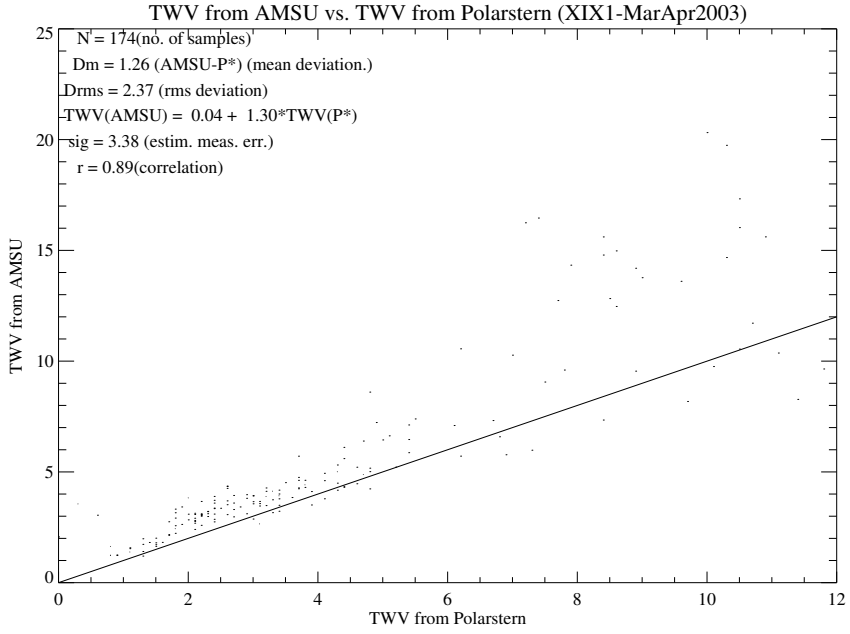

Figure 4: AMSU-B-derived TWV versus Polarstern radiosonde TWV, March-April 2003 (cruise ARK XIX-1); solid line = identity.

larstern is Vaisala RS80. This radiosonde type is known to have a dry bias in cold conditions [Elliot and Gaffen, 1991], i.e., it then underestimates humidity.

2.2 Comparison of maps, time evolution

If the retrieved TWV data are plotted as daily average maps (0.5° gridding in latitude and longitude) they can be compared to maps of TWV from NCEP (National Centers for Environmental Prediction). A series of such daily maps, covering about 3 weeks in March 2002, is shown in the appendix. They show rather good qualitative and quantitative agreement. Particularly interesting is the propagation of humid air masses (TWV above 7 kg/m^2) through the Bering Strait into the central Arctic (upper centre of the maps). This could formerly (i.e., not using the extended algorithm) not be retrieved.

References

S. Buehler, P. Eriksson, T. Kuhn, A. von Engeln, and C. Verdes. ARTS, the atmospheric radiative transfer simulator. *J. Quant. Spectroscopy and Radiative Transfer*, 91:65–93, 2005. doi: 10.1016/j.jqsrt.2004.05.051.

R. Elliot and G. Gaffen. On the utility of radiosonde humidity archives for climate studies. *Bull. Am. Meteorol. Soc.*, 72:1507–1520, 1991.

S. English and T. Hewison. A fast generic millimetre wave emissivity model. *Proceedings of SPIE*, 3503:288–300, 1998.

A. Guissard and P. Sobieski. A simplified radiative transfer equation for application in ocean microwave remote sensing. *Radio Sci.*, 29(4):881–894, 1994.

M. Janssen, editor. *Atmospheric Remote Sensing by Microwave Radiometry*. John Wiley and Sons, New York, 1993. 572 pp.

J. Miao. *Retrieval of Atmospheric Water Vapor Content in Polar Regions Using Spaceborne Microwave Radiometry*. Reports on Polar Research 289/1998. Alfred-Wegener Institute for Polar and Marine Research, Bremerhaven, Germany, 1998. 109 pp.

J. Miao, K. F. Knzi, G. Heygster, T. A. Lachlan-Cope, and J. Turner. Atmospheric water vapor over Antarctica derived from SSM/T2 data. *J. Geophys. Res.*, 106(D10):10187–10203, 2001.

N. Selbach. *Determination of Total Water Vapour and Surface Emissivity of Sea Ice at 89 GHz, 157 GHz and 183 GHz in the Arctic winter*. Berichte aus dem Institut fr Umweltphysik, Vol. 21. Logos-Verlag, Berlin, Germany, 2003. PhD thesis, 191 pp.

A Total water vapour maps of the arctic and subarctic regions, from AMSU-B data and from NCEP reanalysis data.

The maps on the left have been derived from AMSU-B data with the extended algorithm described above, the ones on the right are maps from NCEP reanalysis data. Grey areas in the maps on the left denote areas where TWV could not be retrieved, mainly because it was too high. Note that the upper TWV limit for retrieval with the extended algorithm is about 7 kg/m^2 over water and land, and about 15 kg/m^2 over sea ice.

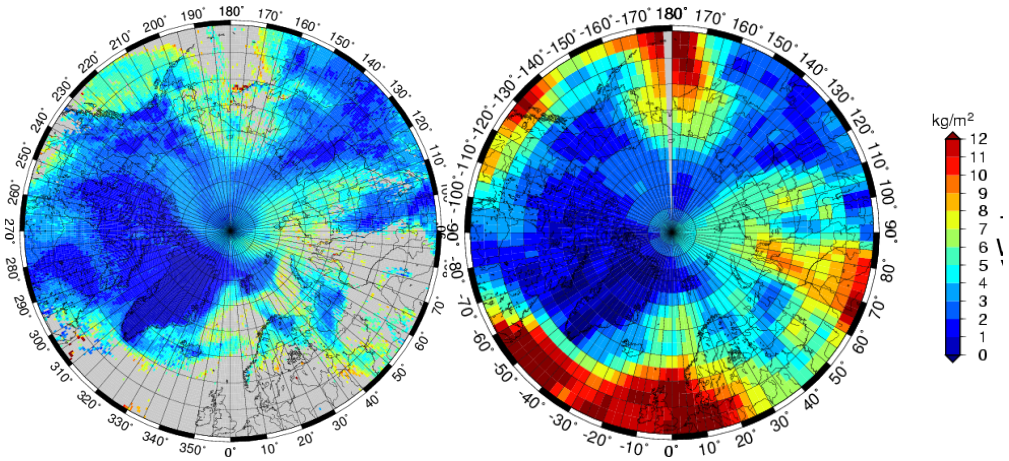

4 March, 2002. Left: from AMSU-B, right: NCEP.

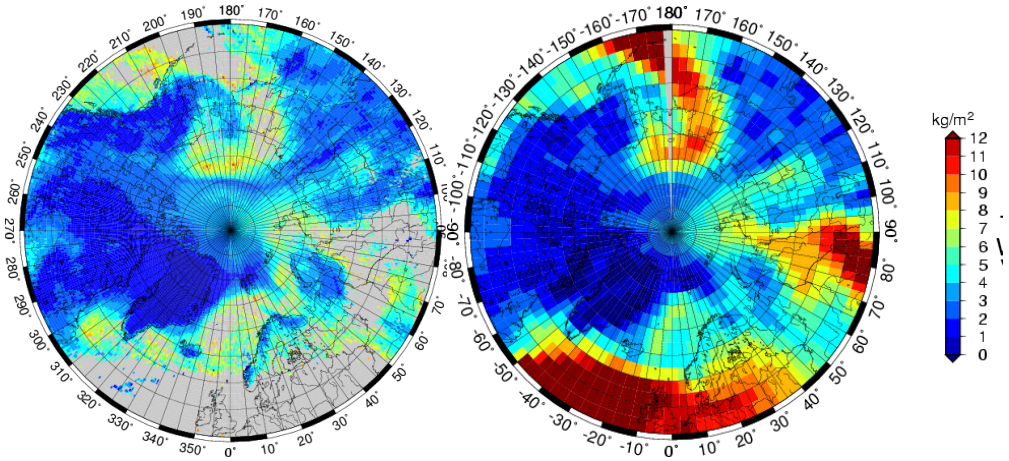

5 March, 2002. Left: from AMSU-B, right: NCEP.

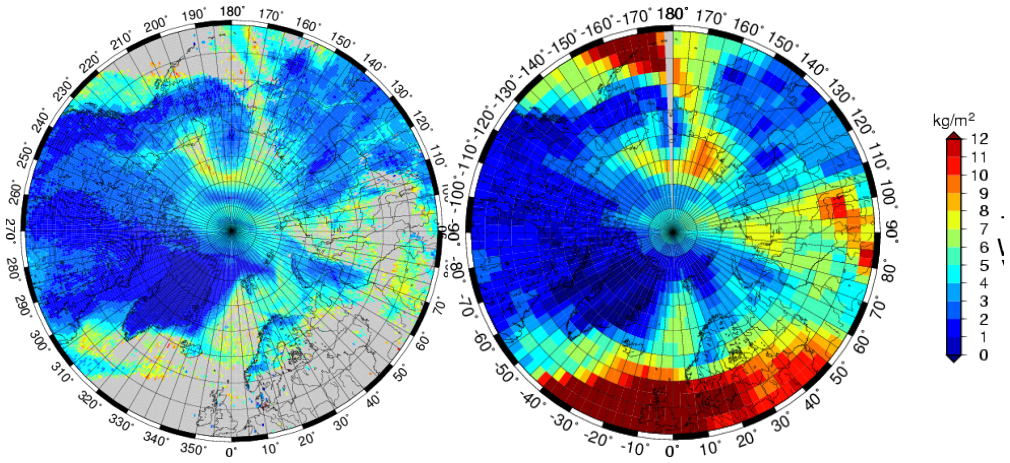

6 March, 2002. Left: from AMSU-B, right: NCEP.

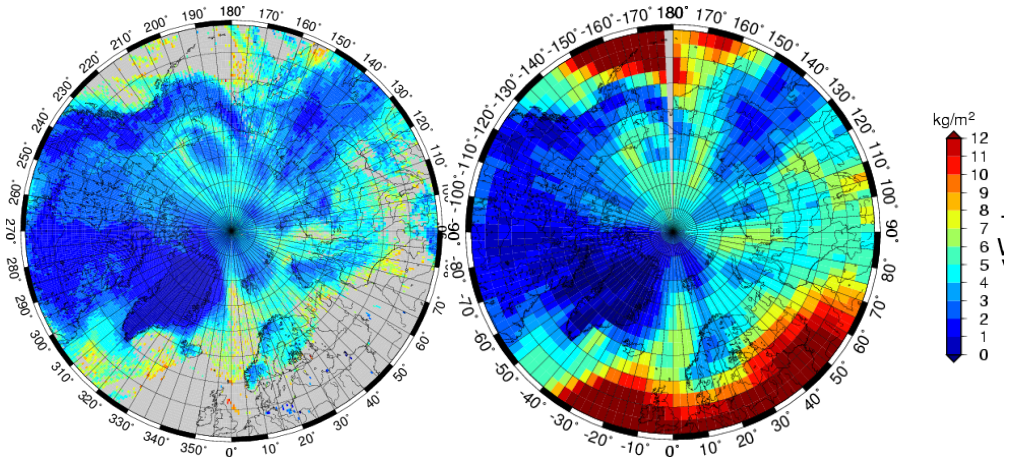

7 March, 2002. Left: from AMSU-B, right: NCEP.

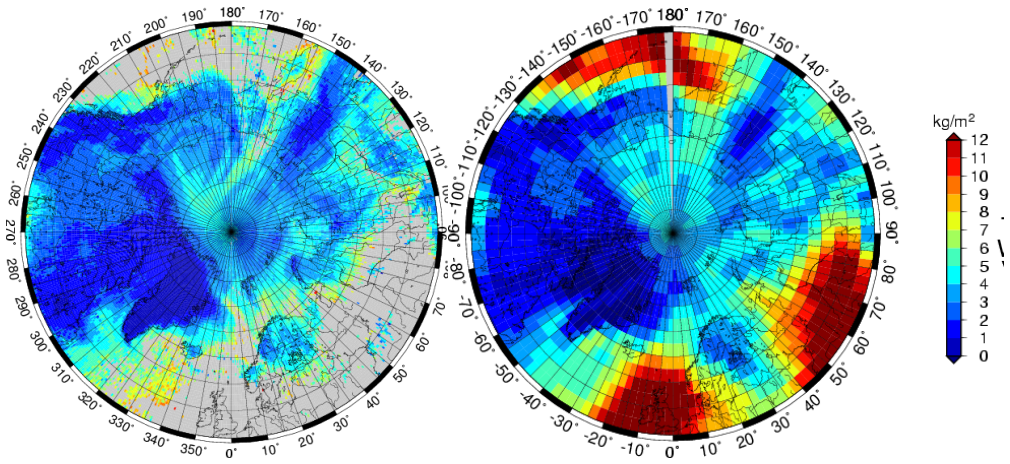

8 March, 2002. Left: from AMSU-B, right: NCEP.

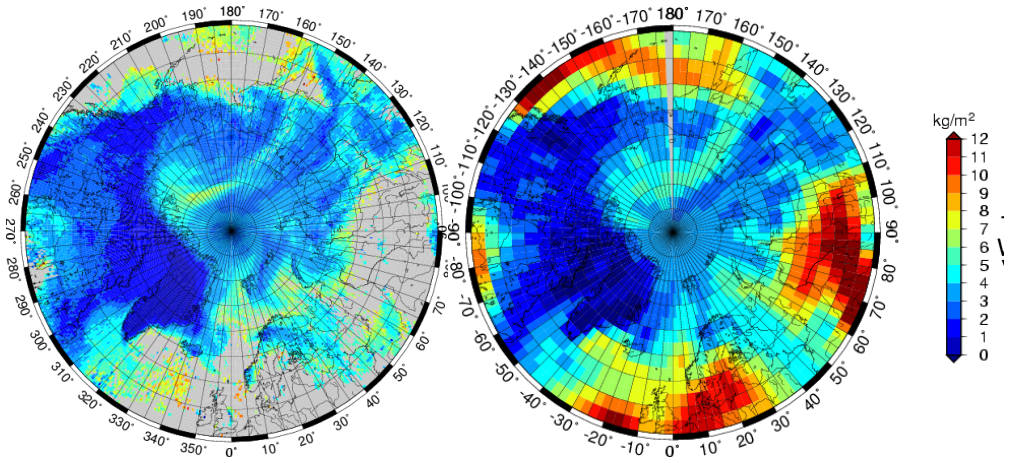

9 March, 2002. Left: from AMSU-B, right: NCEP.

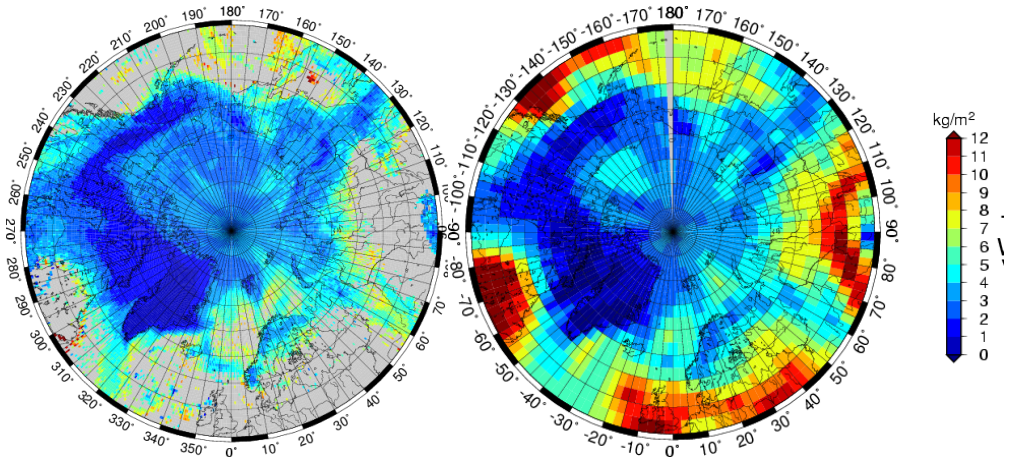

10 March, 2002. Left: from AMSU-B, right: NCEP.

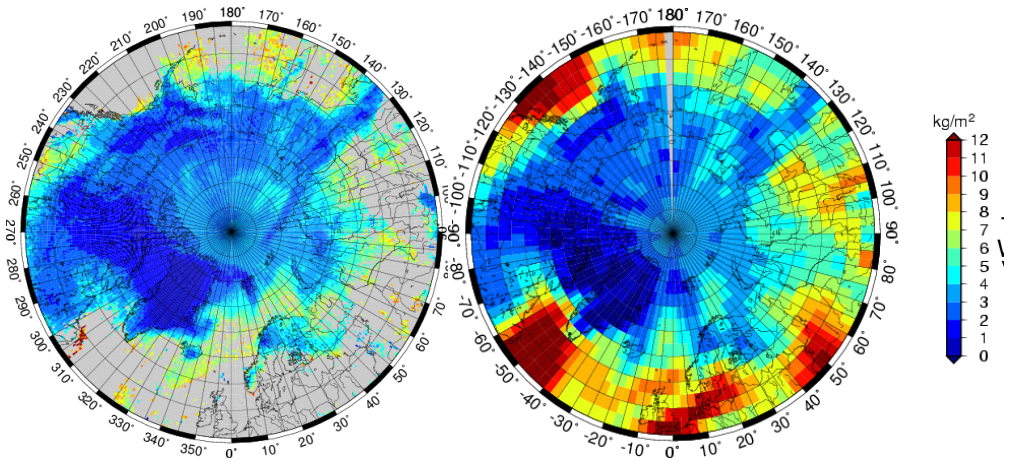

11 March, 2002. Left: from AMSU-B, right: NCEP.

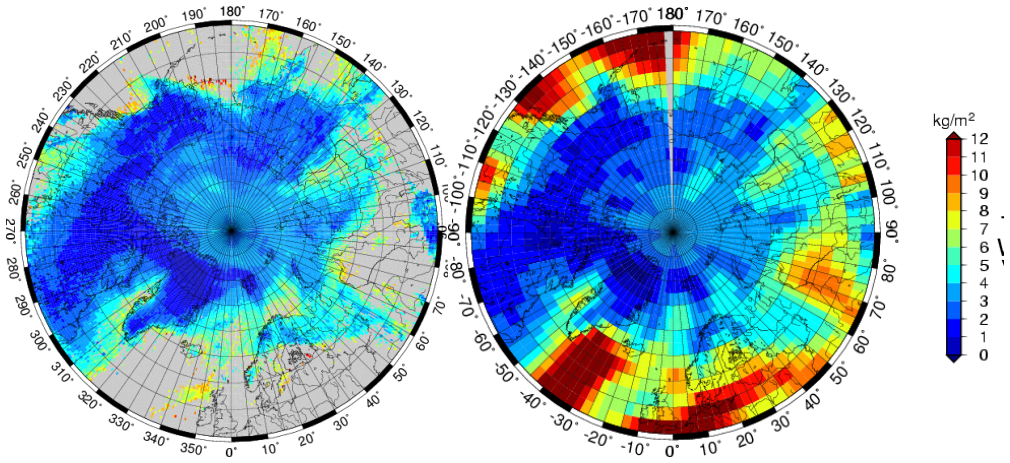

12 March, 2002. Left: from AMSU-B, right: NCEP.

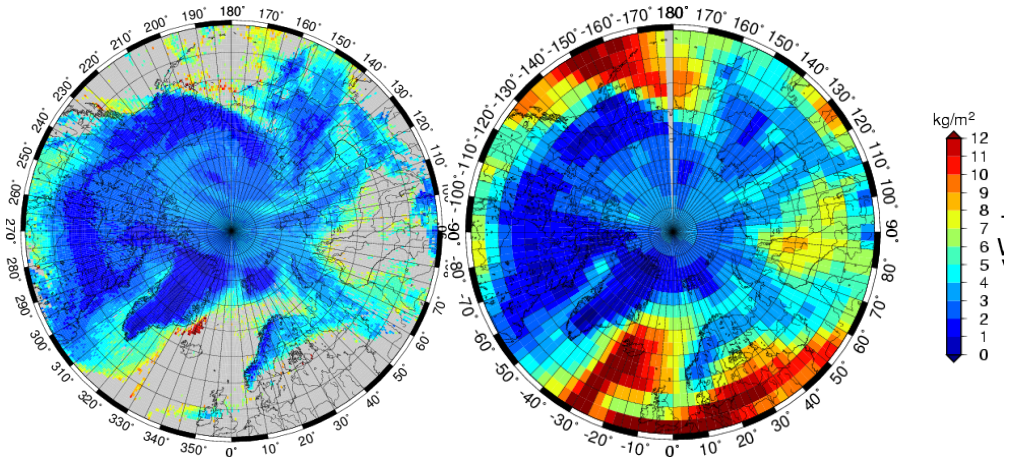

13 March, 2002. Left: from AMSU-B, right: NCEP.

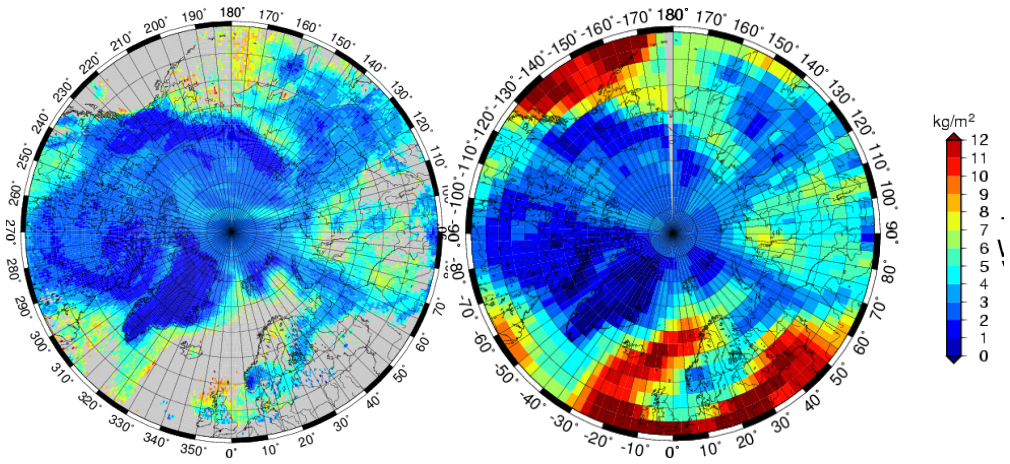

14 March, 2002. Left: from AMSU-B, right: NCEP.

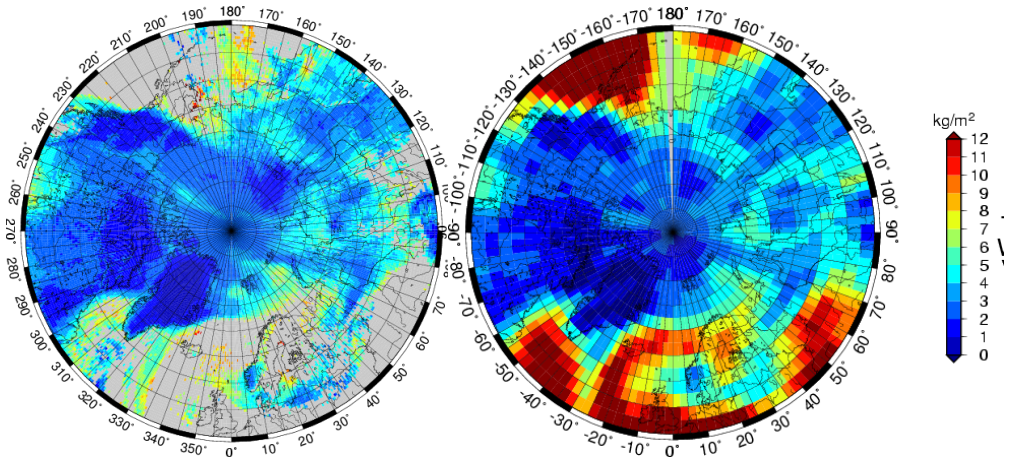

15 March, 2002. Left: from AMSU-B, right: NCEP.

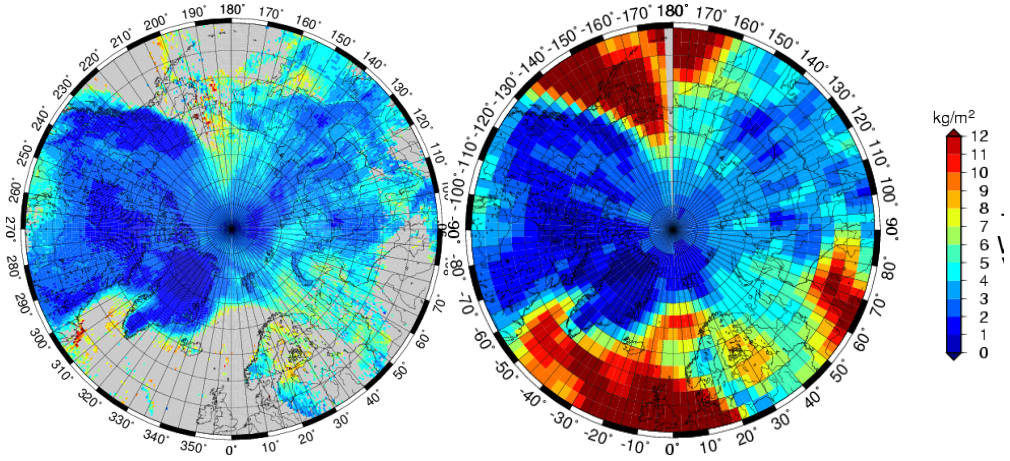

16 March, 2002. Left: from AMSU-B, right: NCEP.

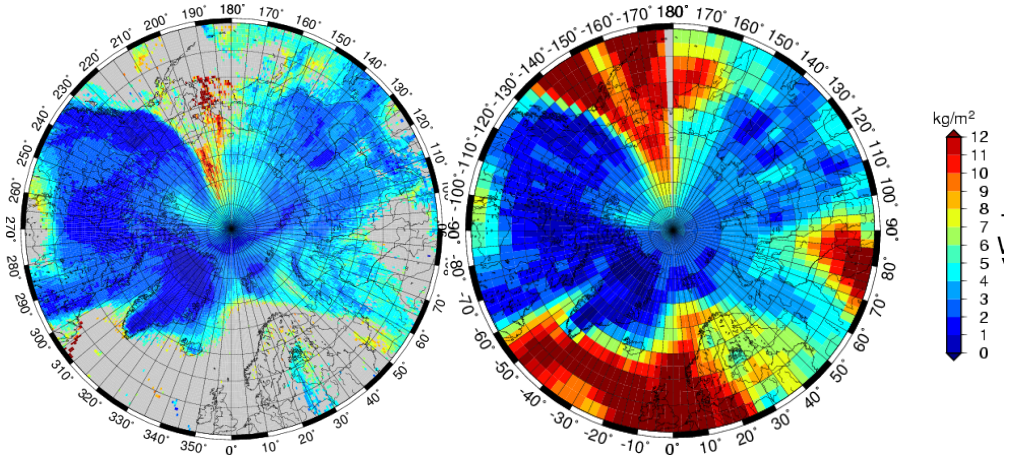

17 March, 2002. Left: from AMSU-B, right: NCEP.

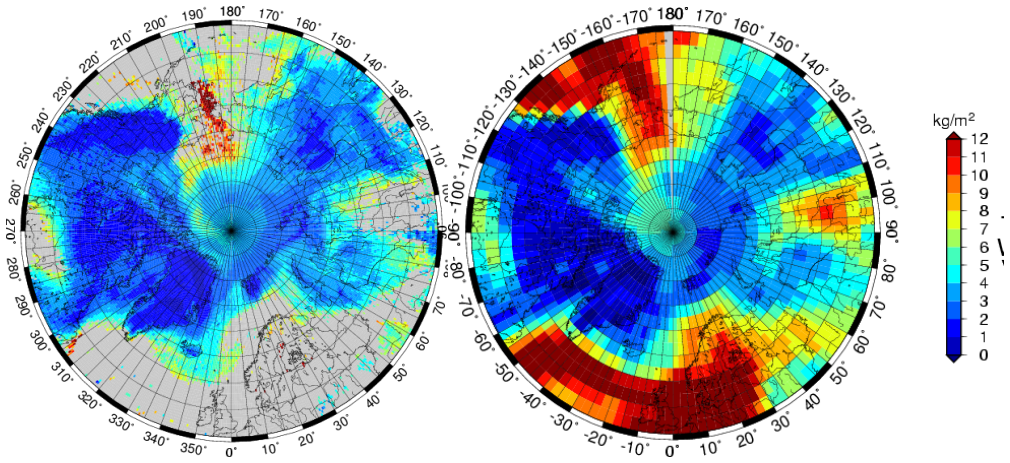

18 March, 2002. Left: from AMSU-B, right: NCEP.

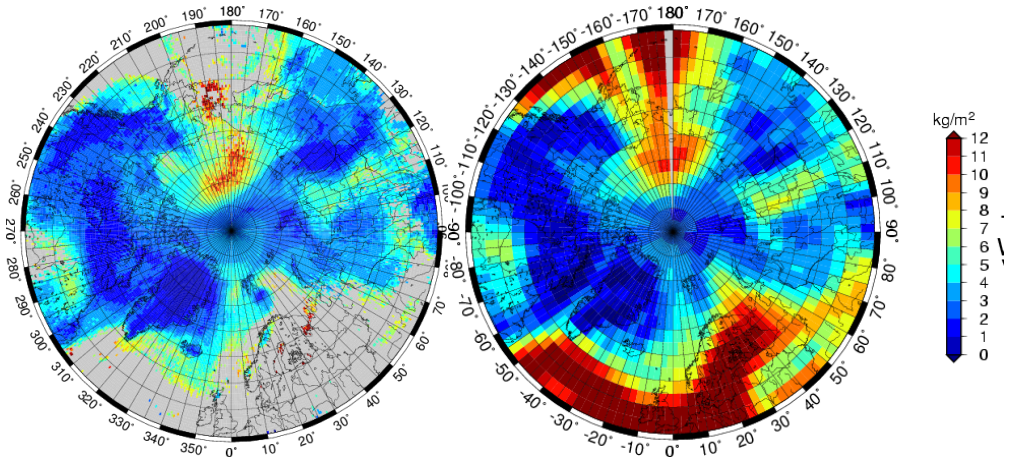

19 March, 2002. Left: from AMSU-B, right: NCEP.

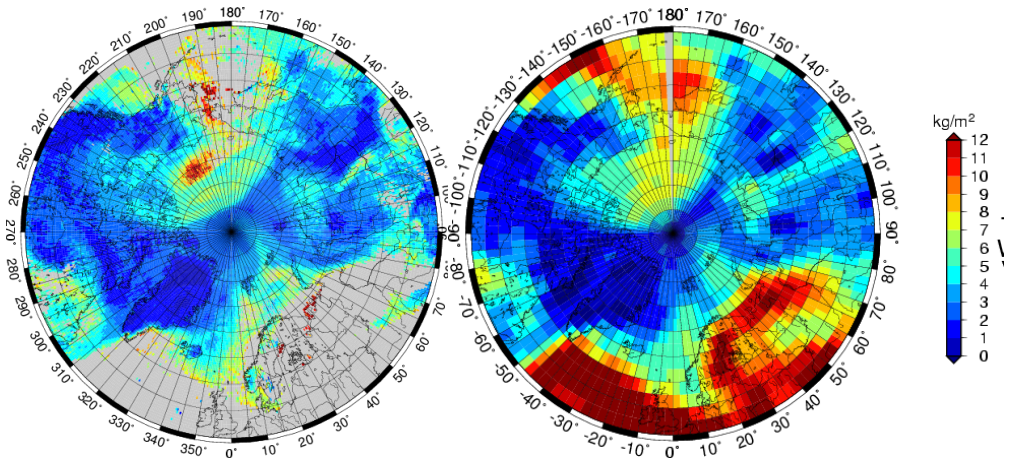

20 March, 2002. Left: from AMSU-B, right: NCEP.

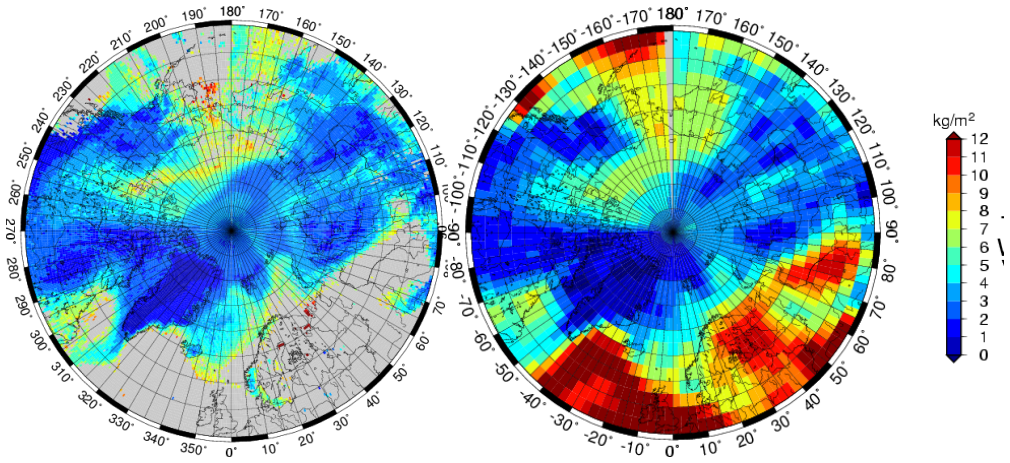

21 March, 2002. Left: from AMSU-B, right: NCEP.

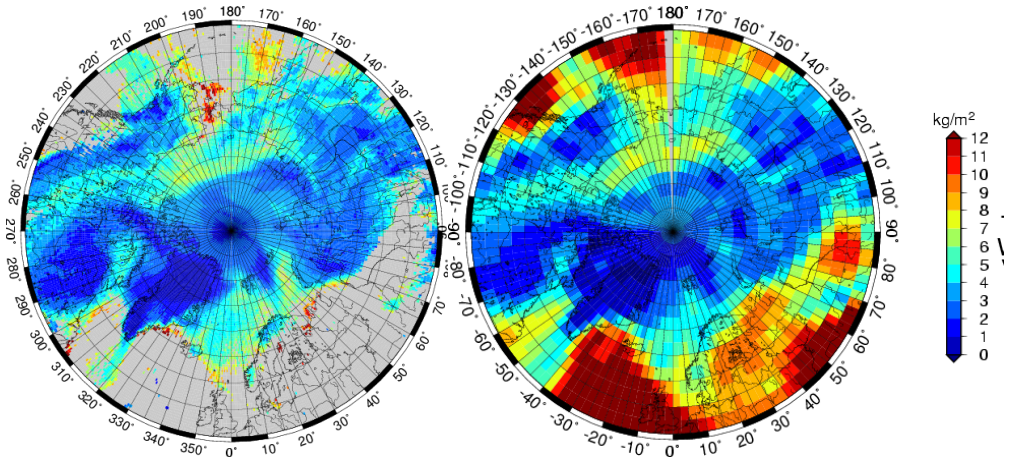

22 March, 2002. Left: from AMSU-B, right: NCEP.

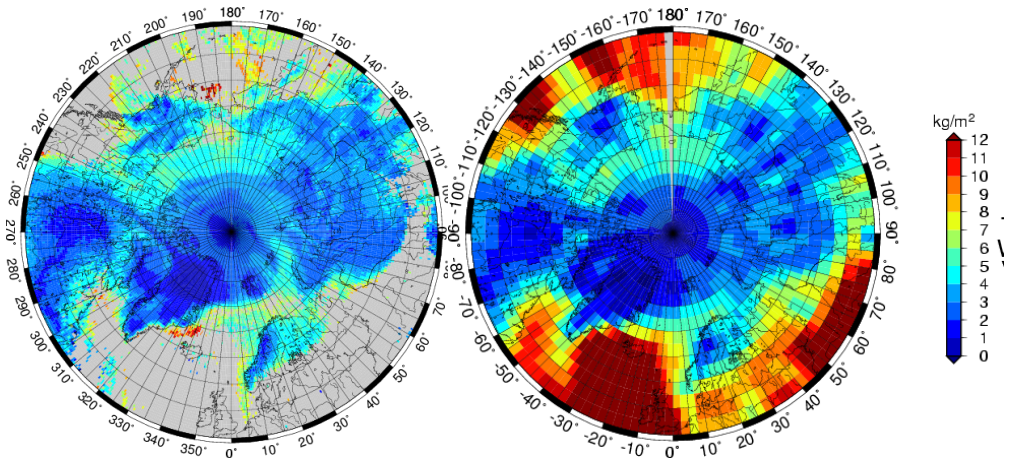

23 March, 2002. Left: from AMSU-B, right: NCEP.

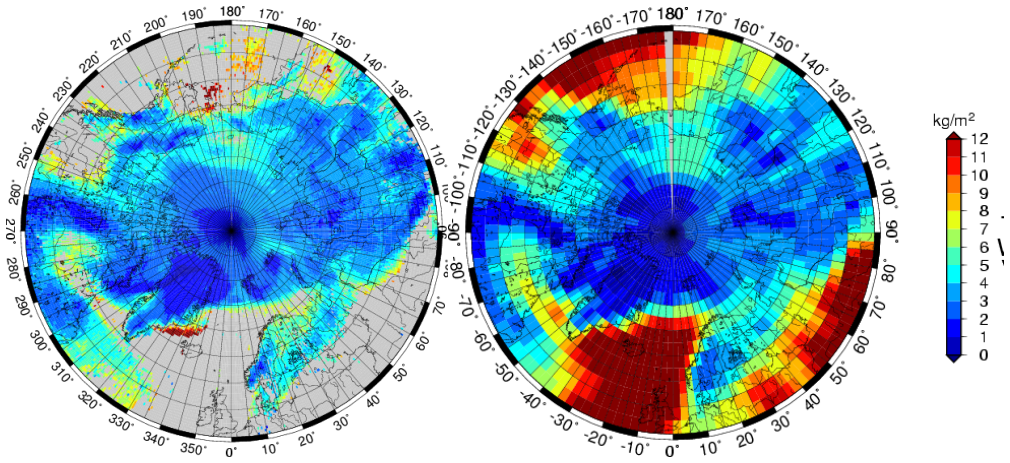

24 March, 2002. Left: from AMSU-B, right: NCEP.

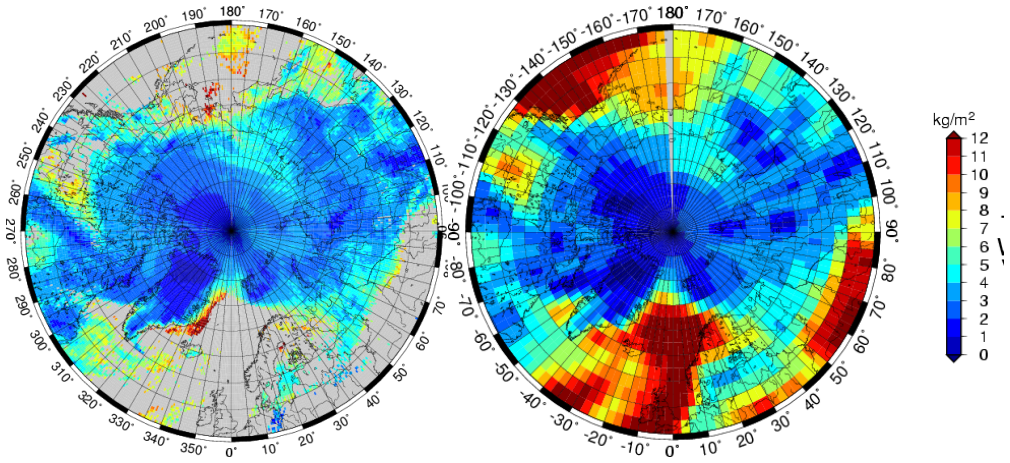

25 March, 2002. Left: from AMSU-B, right: NCEP.

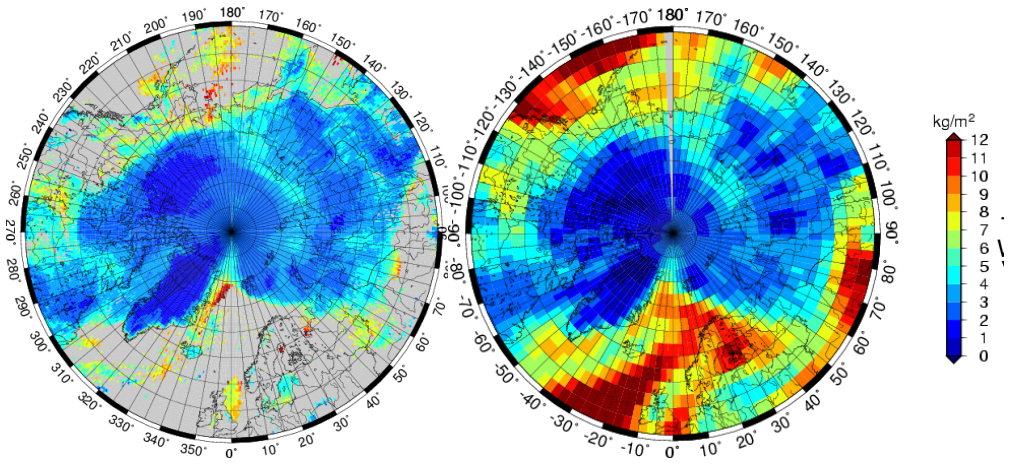

26 March, 2002. Left: from AMSU-B, right: NCEP.

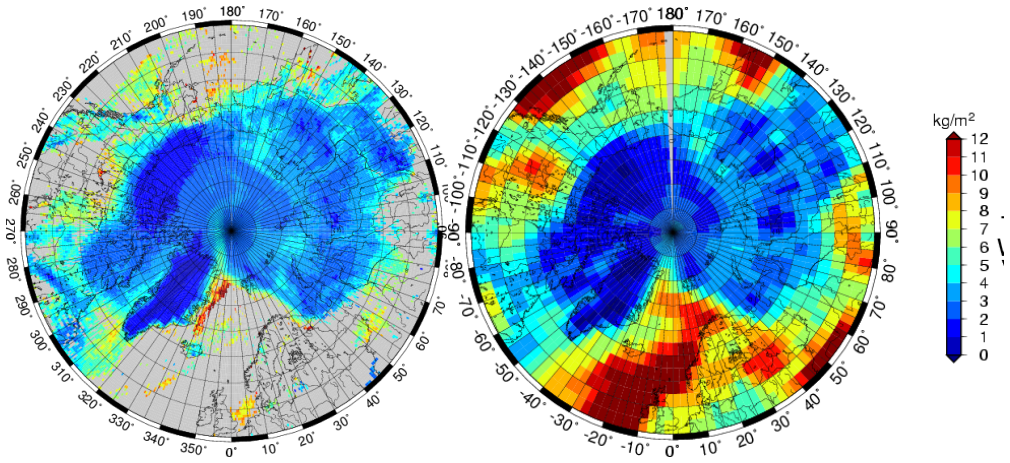

27 March, 2002. Left: from AMSU-B, right: NCEP.

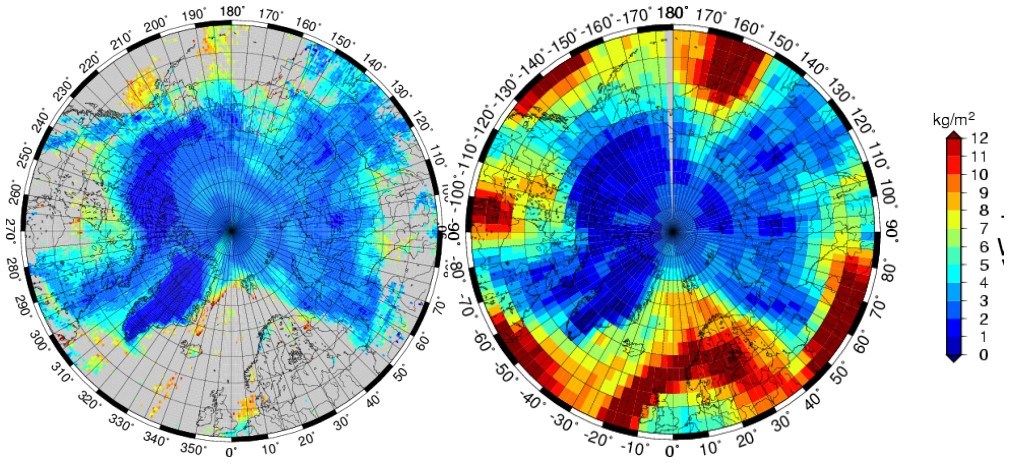

28 March, 2002. Left: from AMSU-B, right: NCEP.

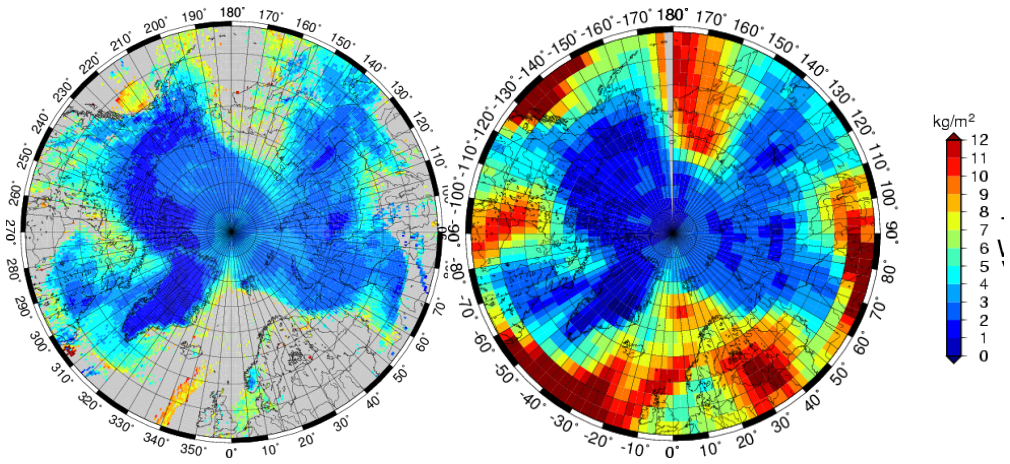

29 March, 2002. Left: from AMSU-B, right: NCEP.

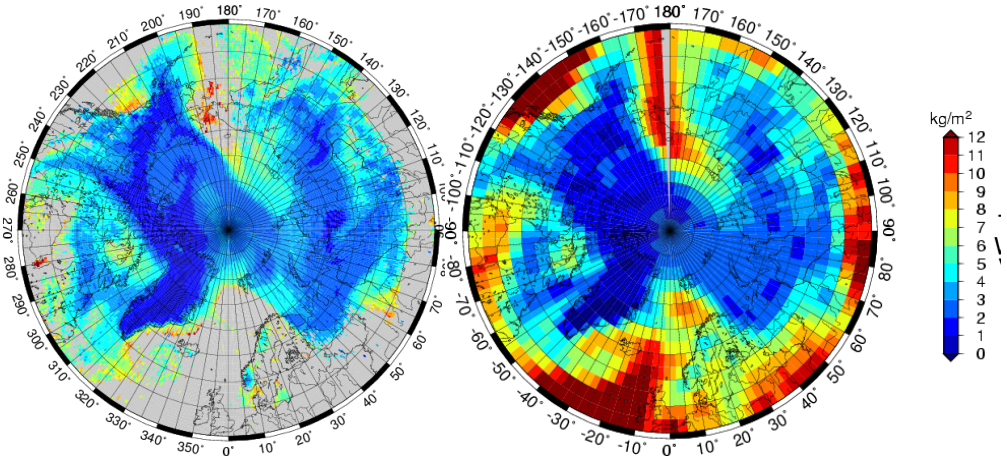

30 March, 2002. Left: from AMSU-B, right: NCEP.

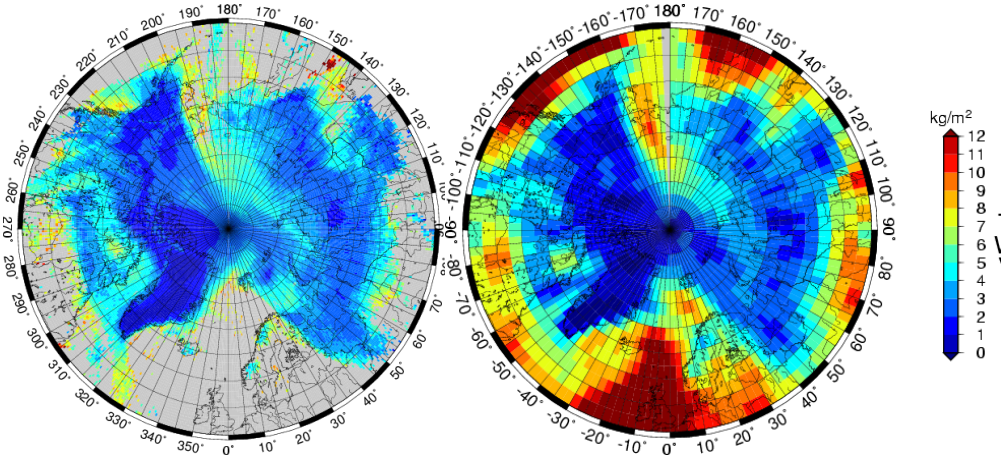

31 March, 2002. Left: from AMSU-B, right: NCEP.